A&A 488, 667–674 (2008)
DOI: 10.1051/0004-6361:200810080

Astronomy & Astrophysics

The radii of the nearby K5V and K7V stars 61 Cygni A & B

CHARA/FLUOR interferometry and CESAM2k modeling

P. Kervella[1], A. Mérand[2], B. Pichon[3], F. Thévenin[3], U. Heiter[4], L. Bigot[3], T. A. ten Brummelaar[2], H. A. McAlister[2], S. T. Ridgway[5], N. Turner[2], J. Sturmann[2], L. Sturmann[2], P. J. Goldfinger[2], and C. Farrington[2]

[1] LESIA, Observatoire de Paris, CNRS UMR 8109, UPMC, Université Paris Diderot, 5 place Jules Janssen, 92195 Meudon, France
e-mail: Pierre.Kervella@obspm.fr
[2] Center for High Angular Resolution Astronomy, Georgia State University, PO Box 3965, Atlanta, Georgia 30302-3965, USA
[3] Université de Nice-Sophia Antipolis, Lab. Cassiopée, UMR 6202, Observatoire de la Côte d'Azur, BP 4229, 06304 Nice, France
[4] Department of Physics and Astronomy, Uppsala University, Box 515, 751 20 Uppsala, Sweden
[5] National Optical Astronomy Observatories, 950 North Cherry Avenue, Tucson, AZ 85719, USA

Received 28 April 2008 / Accepted 23 June 2008

ABSTRACT

Context. The main sequence binary star 61 Cyg (K5V+K7V) is our nearest stellar neighbour in the northern hemisphere. This proximity makes it a particularly well suited system for very high accuracy interferometric radius measurements.
Aims. Our goal is to constrain the poorly known evolutionary status and age of this bright binary star.
Methods. We obtained high accuracy interferometric observations in the infrared K′ band, using the CHARA/FLUOR instrument. We then computed evolutionary models of 61 Cyg A & B with the CESAM2k code. As model constraints, we used a combination of observational parameters from classical observation methods (photometry, spectroscopy) as well as our new interferometric radii.
Results. The measured limb darkened disk angular diameters are $\theta_{\rm LD}$(A) = 1.775 ± 0.013 mas and $\theta_{\rm LD}$(B) = 1.581 ± 0.022 mas, respectively for 61 Cyg A and B. Considering the high accuracy parallaxes available, these values translate into photospheric radii of R(A) = 0.665 ± 0.005 $R_\odot$ and R(B) = 0.595 ± 0.008 $R_\odot$. The new radii constrain efficiently the physical parameters adopted for the modeling of both stars, allowing us to predict asteroseismic frequencies based on our best-fit models.
Conclusions. The CESAM2k evolutionary models indicate an age around 6 Gyr and are compatible with small values of the mixing length parameter. The measurement of asteroseismic oscillation frequencies in 61 Cyg A & B would be of great value to improve the modeling of this important fiducial stellar system, in particular to better constrain the masses.

Key words. stars: individual: 61 Cyg – stars: evolution – stars: fundamental parameters – techniques: interferometric

1. Introduction

Binary stars are numerous in the Galaxy but only few of them can be fully calibrated physically. They are interesting for several reasons, among them the most important for evolutionary modeling is that the two components are coeval, and share the same chemical abundances of the original material. This makes their modeling much easier than for single stars, as several free parameters of the models are shared between the two stars (age and helium content). Possibly the best example of physical calibration of a binary system is provided by our closest neighbour, α Cen (Thévenin et al. 2002). Its two solar-type components were analyzed in detail with the use of photometry, spectrometry, astrometry and interferometry. It resulted in excellent knowledge of the masses of the two components (within less than 1%), and, through modeling of the stars, of fundamental parameters not directly accessible to measurements, like the age or the helium content. Therefore, these two stars are, with Procyon, Sirius and Vega, among the most important benchmark stars for new developments of stellar structure and atmosphere models. The present study focusses on 61 Cyg A (HD 201091, HIP 104214) and B (HD 201092, HIP 104217), the nearest stars in the northern hemisphere. The two stars constitute a visual binary pair with a very long orbital period (≈650 yrs), also known as Gl 820. The parallax of this system was first measured by Bessel (1838), and it is now known with extremely high accuracy. The proper motion of more than 5″ per year, first determined by Piazzi in the XVIIIth century, makes it one of the fastest moving stars in terms of apparent displacement. Although some of this motion comes from the proximity of 61 Cyg to us, the pair has also a high radial velocity of 108 km s^{-1}, indicating that 61 Cyg is not a member of the thin disk of our Galaxy. The proximity of 61 Cyg makes it a northern analog of the numerical modeling benchmark α Cen. Its large parallax also means that this is the easiest low-mass dwarf to resolve interferometrically. The spectral types of its two members (K5V and K7V) ideally complement our previous studies of α Cen A & B (G2V+K1V, Kervella et al. 2003a; Bigot et al. 2006). The masses of 61 Cyg A & B are controversial, with estimates ranging from approximately 0.74 and 0.46 $M_\odot$ (Gorshanov et al. 2006) to 0.67 and 0.59 $M_\odot$ (Walker et al. 1995). With effective temperatures of about 4 400 and 4 000 K, they shine with luminosities of only 0.15 and 0.08 $L_\odot$. There is no confirmed planet around them, although indications exist that 61 Cyg B could host a giant planetary companion (see. Sect. 2.3). As dimmer versions of solar type stars, they have magnetic cycles similar to that of the Sun, the brighter 8 years, the fainter 11 years (Hempelmann et al. 2006). Their rotation periods are of the order of 35 days, therefore no rotational distorsion of their photospheres is expected. The abundances of heavy chemical elements have been determined (Luck & Heiter 2005, 2006) in

Table 1. Calibrators used for the observations. They were selected in the catalogue assembled by Mérand et al. (2005). The limb darkened ($\theta_{\rm LD}$) and uniform disk ($\theta_{\rm UD\,K}$, for the K band) angular diameters are given in milliarcseconds (mas). The angular separation α between the calibrators and 61 Cyg is given in the last column, in degrees.

Star	m_V	m_K	Spect.	$\theta_{\rm LD}$ (mas)	$\theta_{\rm UD\,K}$ (mas)	α (°)
HD 196753	5.94	3.34	K0II-III	1.047 ± 0.013	1.022 ± 0.013	16.2
HD 200451	7.23	2.90	K5III	1.485 ± 0.019	1.441 ± 0.019	12.3

these stars which are found slightly metal poor (−0.2 dex), so a priori older than the Sun but belonging to the galactic disk.

In Sect. 2, we detail the interferometric observations and the corresponding physical parameters we derive (angular diameters and linear radii). Together with the additional observables listed in Sect. 3, we propose in Sect. 4 a modeling of the two stars using the CESAM2k code. We finally present asteroseismic frequency predictions in Sect. 5.

2. Interferometric observations

2.1. Instrumental setup

Our observations of 61 Cyg were undertaken in November 2006 in the near infrared K' band ($1.9 \leq \lambda \leq 2.3$ μm), at the CHARA Array (ten Brummelaar et al. 2005) using FLUOR, the Fiber Linked Unit for Optical Recombination (Coudé du Foresto et al. 2003). We used the FLUOR Data reduction software (DRS) (Coudé du Foresto et al. 1997; Kervella et al. 2004a; Mérand et al. 2006), to extract the squared instrumental visibility of the interference fringes. The baseline was chosen according to the predicted angular sizes of 61 Cyg A & B (approximately 1.5 to 2 mas) and the wavelength of observation, in order to obtain the most constraining measurements on the angular diameters. This led to the choice of the CHARA telescopes S1 and E2, separated by a linear distance of 279 m. The calibrator stars were chosen in the catalogue compiled by Mérand et al. (2005), using criteria defined by these authors (Table 1). They were observed immediately before or after 61 Cyg in order to monitor the interferometric transfer function of the instrument.

We selected these calibrators so that their visibility measurements have comparable signal-to-noise ratios to 61 Cyg A & B. As they have nearly the same effective temperature and brightness as our targets, their angular diameters are also similar. It results that the final precision of our angular diameter measurements of 61 Cyg is limited by the uncertainties on the calibrators' diameters. We took them carefully into account in our final error bars, including the correlations between different calibrated observations of the same star. The reader is referred to Perrin (2003) for a detailed description of the error propagation method we used. The final calibrated visibilites of 61 Cyg A and B are listed in Table 2.

As a remark, using smaller (hence fainter) calibrator stars would have led to a larger observational uncertainty on the measured visibility of the calibrator and would not have improved, or only on a marginal note, the accuracy of the angular diameters of 61 Cyg A & B.

2.2. Limb darkened angular diameters

In order to estimate the angular diameter from the measured visibilities it is necessary to know the intensity distribution of the light on the stellar disk, i.e. the limb darkening (LD). We selected the four-parameter LD law of Claret (2000):

$$I(\mu)/I(1) = 1 - \sum_{k=1}^{4} a_k (1 - \mu^{\frac{k}{2}}). \quad (1)$$

The a_k coefficients are tabulated by this author for a wide range of stellar parameters ($T_{\rm eff}$, $\log g$,...) and photometric bands (U to K). To read Claret's tables for the PHOENIX models, the effective temperatures of 61 Cyg A and B were rounded to $T_{\rm eff}$(A) = 4400 K and $T_{\rm eff}$(B) = 4000 K, with a metallicity rounded to solar ($\log$ [M/H] = 0.0), a turbulent velocity $V_{\rm T}$ = 2 km s^{-1}, and a surface gravity rounded to $\log g$ = 5.0. From the masses we derive in Sect. 4 (listed in Table 5) and the measured radii (Sect. 2.4), the effective gravities are $\log g$ = 4.71 and $\log g$ = 4.67, respectively for 61 Cyg A and B. The values of the four a_i parameters corresponding to Claret's intensity profiles of the two stars in the K band are given in Table 3.

The FLUOR instrument bandpass corresponds to the K' filter ($1.9 \leq \lambda \leq 2.3$ μm). An effect of this relatively large spectral bandwidth is that several spatial frequencies are simultaneously observed by the interferometer. This effect is known as bandwidth smearing. It is usually negligible for $V^2 \geq 40\%$, but not in our case as the measured visibilities are closer to the first

Table 2. Squared visibility measurements obtained for 61 Cyg A & B. B is the projected baseline length, and "PA" is the azimuth of the projected baseline (counted positively from North to East).

MJD	Star	B (m)	PA (°)	$V^2 \pm \sigma(V^2)$
53 540.352	61 Cyg A	210.98	5.35	0.1194 ± 0.0092
53 540.375	61 Cyg A	210.98	0.21	0.1381 ± 0.0098
53 540.429	61 Cyg A	210.89	−11.70	0.1322 ± 0.0082
53 542.433	61 Cyg A	210.80	−13.88	0.1356 ± 0.0084
54 043.158	61 Cyg A	205.50	−32.51	0.1407 ± 0.0258
54 043.203	61 Cyg A	197.66	−39.53	0.1882 ± 0.0122
54 044.149	61 Cyg A	206.30	−31.35	0.1393 ± 0.0270
54 044.190	61 Cyg A	199.81	−38.07	0.1792 ± 0.0207
54 052.124	61 Cyg A	33.54	−21.29	0.9559 ± 0.0123
54 052.159	61 Cyg A	33.04	−27.24	0.9239 ± 0.0166
54 052.193	61 Cyg A	32.23	−32.48	0.9517 ± 0.0092
54 052.234	61 Cyg A	30.70	−37.98	0.9656 ± 0.0090
54 055.169	61 Cyg A	96.60	72.69	0.6990 ± 0.0107
54 055.211	61 Cyg A	85.78	60.16	0.7427 ± 0.0105
53 540.401	61 Cyg B	210.98	−5.67	0.1714 ± 0.0114
53 540.449	61 Cyg B	210.67	−16.13	0.1840 ± 0.0116
54 043.169	61 Cyg B	204.09	−34.24	0.2982 ± 0.0257
54 044.159	61 Cyg B	205.08	−33.05	0.3049 ± 0.0162
54 044.199	61 Cyg B	197.90	−39.38	0.2694 ± 0.0340
54 049.172	61 Cyg B	231.56	52.54	0.1386 ± 0.0092
54 049.207	61 Cyg B	217.61	41.37	0.1919 ± 0.0098
54 052.135	61 Cyg B	33.41	−23.29	0.9670 ± 0.0168
54 052.171	61 Cyg B	32.80	−29.16	0.9405 ± 0.0140
54 052.208	61 Cyg B	31.76	−34.56	0.9253 ± 0.0144
54 055.180	61 Cyg B	94.08	69.75	0.7731 ± 0.0120
54 055.222	61 Cyg B	82.60	56.28	0.8229 ± 0.0191

Table 3. Limb darkening coefficients of the four-parameter power law of Claret (2000) for 61 Cyg A & B.

Star	a_1	a_2	a_3	a_4
61 Cyg A	0.9189	−0.5554	0.3920	−0.1391
61 Cyg B	1.2439	−1.5403	1.3069	−0.4420

minimum of the visibility function. To account for this effect, the model visibility is computed for regularly spaced wavenumber spectral bins over the K' band, and then integrated to obtain the model visibility. This integral is computed numerically and gives the model V^2 as a function of the projected baseline B and the angular diameter $\theta_{\rm LD}$. A simple χ^2 minimization algorithm is then used to derive $\theta_{\rm LD}$, the 1σ error bars and the reduced χ^2. For more details about this fitting procedure, the reader is referred to Kervella et al. (2003b) or Aufdenberg et al. (2005).

In the infrared K band, the LD is much weaker than in the visible, and for instance the difference in the LD of 61 Cyg A and B is small. It can be quantified by the ratio β of the LD angular diameter $\theta_{\rm LD}$ and the equivalent uniform disk angular diameter $\theta_{\rm UD}$. From Claret's models, we obtain β(A) = 1.0305 and β(B) = 1.0263. The difference between the two stars is 0.4% for $\Delta T_{\rm eff} \approx 400$ K. To account for the uncertainty on the effective temperatures, we thus included a ±0.2% systematic uncertainty on the LD angular diameters of the two stars. The LD being in any case small in the K band, this appears as a reasonable assumption.

There is also an uncertainty on the effective wavelength of the instrument. As the measurements are differential in nature (between the scientific targets and the calibrators), this impacts the measurement only as a second order effect. The true effective wavelength of FLUOR instrument was calibrated by observing with high accuracy the binary star ι Peg (Mérand et al. 2008, in prep.). The relative uncertainty introduced on the angular diameters of 61 Cyg A & B is estimated to ±0.1%, i.e. negligible compared to the statistical uncertainties (0.7% and 1.4%). Both the LD and wavelength uncertainties were added quadratically to the errors from the fitting to arrive at the final uncertainties of the LD angular diameters. The result of the fits are presented for 61 Cyg A & B in Fig. 1. The reduced χ^2 are 1.0 and 3.6, respectively for A and B. From the CHARA/FLUOR visibilities, we derive the following LD angular diameters:

$$\theta_{\rm LD}(61\ {\rm Cyg\ A}) = 1.775 \pm 0.013\ {\rm mas}, \quad (2)$$

$$\theta_{\rm LD}(61\ {\rm Cyg\ B}) = 1.581 \pm 0.022\ {\rm mas}. \quad (3)$$

2.3. Angular diameter discussion

We can compare the measured LD angular diameters to the expected values for these stars from the surface brightness-color relations calibrated by Kervella et al. (2004b). Using the $(B, B-L)$ relation (photometry from Ducati et al. 2002), we obtain the following predicted values: $\theta_{\rm LD}$(61 Cyg A) = 1.813 ± 0.019 mas, and $\theta_{\rm LD}$(61 Cyg B) = 1.704 ± 0.018 mas. While the agreement is good for A (within $\approx 1\,\sigma$), the predicted size for B is $4\,\sigma$ larger than the measured value. Both our measured angular diameter value for 61 Cyg B and this estimate from surface brightness are significantly different from the measurement obtained by Lane & Colavita (2003) using the Palomar Testbed Interferometer. They obtained an angular diameter of $\theta_{\rm LD}$(61 Cyg B) = 1.94 ± 0.009 mas, that corresponds to a difference of $+8\,\sigma$ from our CHARA/FLUOR measurement, and $+11\,\sigma$ from the surface brightness predicted values. One should note that the measurement of the angular size of the star was not the primary focus of their work (in particular, no spatial filter was used for this measurement, resulting in a more difficult calibration of the visibilities).

These discrepancies combine with the larger observed dispersion of the CHARA/FLUOR measurements (compared to A) to indicate a possible additional contributor in the interferometric field of view around B (≈1"). Moreover, 61 Cyg B shows a slight visibility deficit at our shortest baseline which corresponds to a 1.0 ± 0.4% photometric excess. These observations can be explained if B is surrounded by a disk, or by the presence of a faint companion. Interestingly, an 8 M_J companion was proposed by Strand (1943, 1957), based on astrometric measurements. This possibility was suggested again by Deich & Orlova (1977), Deich (1978), and recently by Gorshanov et al. (2006), based on astrometry of the two stars. One should note however that a giant planet with a mass around 10 M_J and the age of 61 Cyg will be extremely faint, according for instance to the models by Baraffe et al. (2003), with an absolute K band magnitude of $M_K \approx 30$, and an apparent magnitude of $m_K \approx 28$. It thus appears unlikely that such a planet can influence the CHARA/FLUOR interferometric measurements. Moreover, using radial velocimetry, Walker et al. (1995) excluded the presence of low mass companions around both components of 61 Cyg down to a few Jupiter masses, up to periods of about 30 years.

As our present data set is too limited to investigate this possibility, we postpone this dicussion to a forthcoming paper. The dispersion of the V^2 measurements observed on B is in any case taken into account in the bootstrapped error bars of the LD angular diameters and will therefore not affect our modeling anaysis.

2.4. Linear photospheric radii

We assumed the following parallax values for the two stars:

$$\pi(61\ {\rm Cyg\ A}) = 286.9 \pm 1.1\ {\rm mas}, \quad (4)$$

$$\pi(61\ {\rm Cyg\ B}) = 285.4 \pm 0.7\ {\rm mas}. \quad (5)$$

They are taken respectively from van Altena et al. (1995) and the *Hipparcos* catalogue (ESA 1997). As a remark, van de Kamp (1973) obtained slightly different values ($\pi_{\rm A} = 282.8 \pm 1.3$ mas and $\pi_{\rm B} = 288.4 \pm 1.6$ mas) using photographic plates collected over the 1912–1972 period (see also van de Kamp 1953). From the reprocessing of the original *Hipparcos* measurements, Van Leeuwen (2007a,b) obtained the following parallaxes: $\pi_{\rm A} = 286.8 \pm 6.8$ mas and $\pi_{\rm B} = 285.9 \pm 0.6$ mas, compatible with our assumed values.

From the combination of the limb darkened angular diameters and trigonometric parallaxes, we derive the following photospheric linear radii:

$$\mathrm{R}(61\ {\rm Cyg\ A}) = 0.665 \pm 0.005\ R_\odot, \quad (6)$$

$$\mathrm{R}(61\ {\rm Cyg\ B}) = 0.595 \pm 0.008\ R_\odot. \quad (7)$$

The relative uncertainties on the radii are therefore ±0.8% and ±1.4% respectively for A and B. Thanks to the high precision of the parallaxes (0.38% and 0.25%), the radius accuracy is limited by the precision of the LD angular diameter measurements.

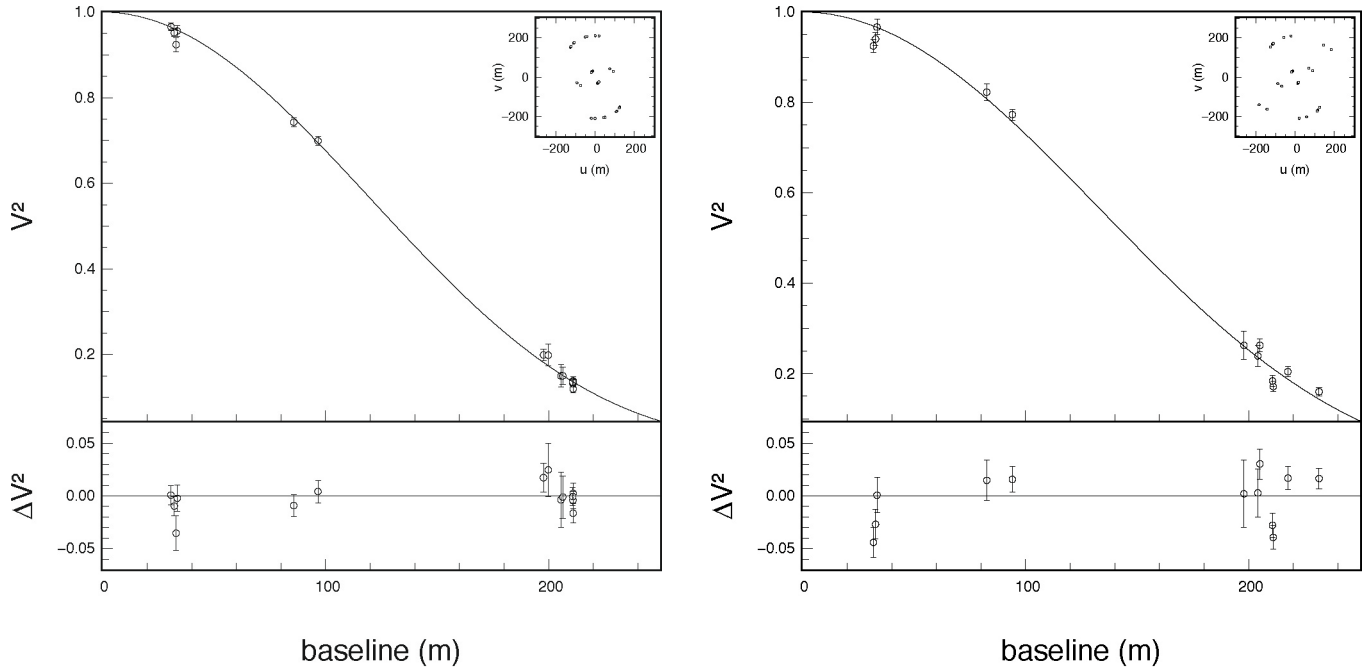

Fig. 1. Visibility data and adjusted limb darkened disk model visibility curve for 61 Cyg A (*left*) and B (*right*) (see also Table 2).

3. Additional observational constraints

3.1. Masses

In spite of the proximity and large semi-major axis (a = 24.65″) of 61 Cyg, its very long orbital period of 6–7 centuries makes it very difficult to determine accurate dynamical masses. Quoting Zagar (1934), Baize (1950) reports a period of 692 years, while Cester et al. (1988) quote a period of 720 yrs and equal masses around 0.5 ± 0.1 $M_\odot$ for both components. Van de Kamp (1954) proposed masses of 0.58 and 0.54 $M_\odot$ for 61 Cyg A and B, respectively. From the orbit determined by Worley & Heintz (1983), Walker et al. (1995) quote masses of:

$$M(61\,\mathrm{Cyg\,A}) = 0.67\,M_\odot, \quad (8)$$

$$M(61\,\mathrm{Cyg\,B}) = 0.59\,M_\odot. \quad (9)$$

While these values are rather uncertain, we will use them as our starting guesses for the CESAM2k modeling. As a comparison, the masses proposed by Gorshanov et al. (2006) of $M(61\,\mathrm{Cyg\,A}) = 0.74 \pm 0.13\,M_\odot$ and $M(61\,\mathrm{Cyg\,B}) = 0.46 \pm 0.07\,M_\odot$ have a larger ratio, although the total mass of the system ($M_{\mathrm{A+B}} = 1.20 \pm 0.15\,M_\odot$) is compatible with Walker et al.'s value.

3.2. Effective temperature

Knowing the LD angular diameter of the stars, it is possible to invert the surface brightness-color (SBC) relations calibrated by Kervella et al. (2004b) to retrieve the effective temperature of a star from any of its apparent magnitudes. Applying this method to 61 Cyg A and B (Fig. 2) yields consistent effective temperatures for the *BVRI* bands of:

$$T_{\mathrm{eff}}(61\,\mathrm{Cyg\,A}) = 4400 \pm 100\,\mathrm{K}, \quad (10)$$

$$T_{\mathrm{eff}}(61\,\mathrm{Cyg\,B}) = 4040 \pm 80\,\mathrm{K}. \quad (11)$$

Table 4. Apparent magnitudes of 61 Cyg A and B from ESA (1997) and Ducati (2002). The uncertainties that were not available were set arbitrarily to ±0.05 mag.

Band	61 Cyg A	61 Cyg B
U	7.48 ± 0.06	8.63 ± 0.05
B	6.27 ± 0.03	7.36 ± 0.02
V	5.20 ± 0.03	6.05 ± 0.01
R	4.17 ± 0.06	4.87 ± 0.05
I	3.52 ± 0.06	4.05 ± 0.05
J	3.10 ± 0.05	3.55 ± 0.02
H	2.48 ± 0.08	2.86 ± 0.04
K	2.35 ± 0.03	2.71 ± 0.05
L	2.28 ± 0.06	2.61 ± 0.05

The apparent magnitudes of the two stars (Table 4) were taken from the *Hipparcos* catalogue (ESA 1997) and the catalogue compiled by Ducati (2002). Thanks to the proximity of 61 Cyg, we can neglect interstellar extinction. As a remark, the average effective temperature retrieved from the *HKL* bands are higher than from the visible bands, respectively by 80 and 200 K for 61 Cyg A and B. It may be a consequence of the activity of the stars, but more likely, it could be due to the relatively poor photometry available in these bands. The two stars are in particular too bright to have accurate magnitudes in the 2MASS catalogue (Skrutskie et al. 2006). For this reason, we consider the T_{eff} estimates based on the visible photometry (*BVRI*) more reliable. The temperatures derived from the *J* band are however in good agreement with these average values. The derived temperatures are identical, within their statistical uncertainties, to those computed from the temperature scale of Alonso, Arribas & Martínez-Roger (1996): 4340 K and 3980 K.

For comparison, Luck & Heiter (2005) determined higher values of T_{eff} = 4640 K and 4400 K for 61 Cyg A and B from spectroscopy. More generally, different techniques result in significantly different T_{eff} values for 61 Cyg A and B, and discrepancies as large as 300 K are found in the literature. This may be a consequence of the activity of the two stars (see

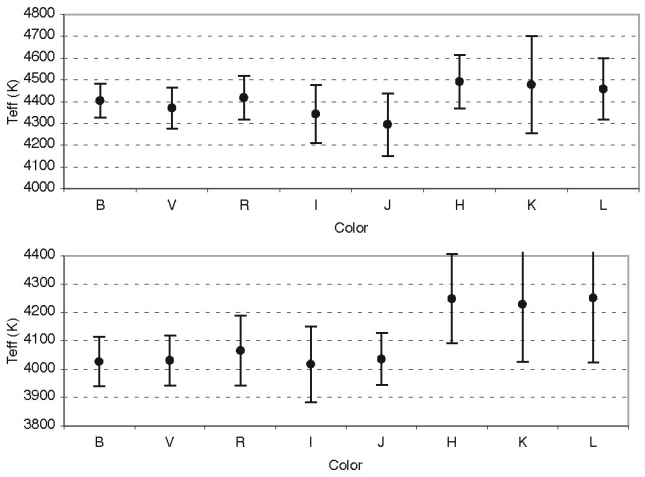

Fig. 2. Effective temperature estimates for 61 Cyg A (*top*) and B (*bottom*) based on their apparent magnitudes and the surface brightness-color relations by Kervella et al. (2004b).

e.g. Hall et al. 2007). 61 Cyg A is also classified as a BY Dra type variable, showing a low amplitude rotational modulation of its light curve due to star spots and chromospheric activity (Böhm-Vitense 2007).

3.3. Luminosity

The luminosity of the two stars of 61 Cyg can be computed using two methods: (1) combining the effective temperature and the interferometric radius; (2) from the apparent magnitude, the bolometric correction, and the parallax.

From the effective temperatures listed in Sect. 3.2 and the radii measured with CHARA/FLUOR (Sect. 2.4), a straightforward application of Stefan-Boltzmann's law ($L = 4\pi R^2 \sigma T_{\rm eff}^4$) gives $L(61\,\mathrm{Cyg\,A}) = 0.149 \pm 0.006\,L_\odot$, and $L(61\,\mathrm{Cyg\,B}) = 0.085 \pm 0.004\,L_\odot$.

We can also use the K band bolometric corrections (BC_K) from Houdashelt et al. (2000) to retrieve the bolometric magnitude from the apparent K band magnitudes of the stars (Table 4). An interpolation of Houdashelt et al.'s tables gives $\mathrm{BC}_K(A) = 2.152$ and $\mathrm{BC}_K(B) = 2.433$. Considering the uncertainty on the metallicity of the two stars, and the difference observed between the visible and infrared effective temperature estimates (Sect. 3.2), we attributed a ±0.07 mag error bar to these bolometric corrections. Together with the parallaxes, they correspond to absolute bolometric magnitudes of $M_{\rm bol}(A) = 6.80 \pm 0.08$ and $M_{\rm bol}(B) = 7.42 \pm 0.09$, and the following luminosities (with $M_{\rm bol}(\odot) = 4.75$):

$$L(61\,\mathrm{Cyg\,A}) = 0.153 \pm 0.010\,L_\odot, \quad (12)$$

$$L(61\,\mathrm{Cyg\,B}) = 0.085 \pm 0.007\,L_\odot. \quad (13)$$

These figures are in excellent agreement with those computed from the effective temperature and the radius. In our subsequent modeling of the two stars, we will use simultaneously as constraints the different available observables. However, various correlations exist between these observables, for instance between R, L and $T_{\rm eff}$ through Stefan-Boltzmann's law, and we prefer to limit the influence of these correlations as much as possible. However, this was not possible with all parameters as, for instance, the parallax plays a role in the derivation of most of them. As the bolometric corrections have the advantage of being independent from the radius measurement, we retain them for our modeling of the two stars.

Table 5. Observational constraints (upper part), and best-fit parameters derived from our CESAM2k modeling of 61 Cyg A & B (lower part). See text for the corresponding references.

Parameter	61 Cyg A	61 Cyg B
π (mas)	286.9 ± 1.1	285.4 ± 0.7
[Fe/H]	−0.20 ± 0.10	−0.27 ± 0.19
$R(R_\odot)$	0.665 ± 0.005	0.595 ± 0.008
$T_{\rm eff}$ (K)	4 400 ± 100	4 040 ± 80
L ($L_\odot$)	0.153 ± 0.010	0.085 ± 0.007
Initial He content $Y_{\rm ini}$	0.265	0.265
Initial [Z/H] (dex)	−0.10	−0.10
Final [Z/H] (dex)	−0.15	−0.15
Age (Gyr)	6.0 ± 1.0	6.0 ± 1.0
Mass ($M_\odot$)	0.690	0.605
α (MLT convection)	1.2	0.8

3.4. Metallicity

An error of 0.10 dex on the metallicity translates into an error of 160 K on the effective temperature, so a good knowledge of the metallicity is important.

A number of metallicity estimates can be found in the literature. Zboril & Byrne (1998) determined the metallicity of 61 Cyg A to be [M/H] = −0.3 ± 0.2, from high-resolution spectroscopy and LTE atmosphere models. They also found a mean metallicity index [M/H] = −0.2 for a sample of 18 K and M field stars. Tomkin & Lambert (1999) obtained relatively low iron abundances of [Fe/H] = −0.43 ± 0.10 for 61 Cyg A and [Fe/H] = −0.63 ± 0.10 for 61 Cyg B, based on equivalent line widths and LTE model atmospheres. Using a similar method, Affer et al. (2005) measured [Fe/H] = −0.37 ± 0.19. for 61 Cyg A.

For the present study, we choose to rely on the work by Luck & Heiter (2005), who determined:

$$[\mathrm{Fe/H}]\,(61\,\mathrm{Cyg\,A}) = -0.20 \pm 0.10 \quad (14)$$

$$[\mathrm{Fe/H}]\,(61\,\mathrm{Cyg\,B}) = -0.27 \pm 0.19. \quad (15)$$

For the abundance analysis, they used plane-parallel, line-blanketed, flux-constant, LTE, MARCS model atmospheres. These models are a development of the programs of Gustafsson et al. (1975). We selected these values, as they are well in line (within 1 to 2σ) with the measurements obtained by other authors. In addition, we used the MARCS models for the atmosphere description of our evolutionary modeling (Sect. 4), so Luck & Heiter's determination appears as a natural choice for consistency.

4. Modeling with CESAM2k

The observational constraints and parameters used to construct our CESAM2k evolutionary models (Morel 1997; Morel & Lebreton 2007) are summarized in Table 5.

As a binary system, components A and B of 61 Cyg must have the same age, initial helium content, and metallicity (assuming that the system formed as a binary). By comparison with our previous modeling efforts (see e.g. Thévenin et al. 2005), we implemented a few modifications for the present work. The equation of state now includes Coulomb corrections due to low

masses of these stars and the corresponding high density. We used MARCS models (Gustafsson et al. 2003, 2007, 2008)[1] for the atmosphere description. The treatment of convection makes use of a new modified routine (conv_a0) based on the classical mixing length theory (hereafter MLT). The mixing length vanishes at the limit between convective and radiative zones[2]. Note that our small values of the α parameter (that describes the convection in MLT) are in good agreement with the systematic trend of this parameter in low mass stars, where its value decreases steeply with mass. For instance, if for the Sun the most common quoted value of α is about 1.9 (Morel et al. 1999), Yildiz et al. (2006) obtain for low mass stars values such as 1.2 for 0.8 $M_\odot$ or 1.7 for 0.9 $M_\odot$. Compared to these values, our values of α of 0.8 for 61 Cyg B (0.6 $M_\odot$) and 1.2 for 61 Cyg A (0.7 $M_\odot$) appear reasonable.

We define the stellar radius of a model as the bolometric one, which is equivalent to the interferometric definition of the limb darkened angular diameter. The microscopic diffusion of chemical species is taken into account according to Burgers (1969), using the resistance coefficients of Paquette et al. (1986). According to the prescription of Morel & Thévenin (2002), we introduce an additional mixing parameterized by Re$\nu \approx 1$. This parameterization is not important for the stars 61 Cyg A & B because the diffusion is inefficient for low mass stars with solar metallicity.

The adopted metallicity [Z/X], which is an input parameter for the evolutionary computations, is given by the iron abundance measured in the atmosphere with the help of the following approximation: $\log(Z/X) \approx [Fe/H] + \log(Z/X)_\odot$. We use the solar mixture of Grevesse & Noels (1993): $(Z/X)_\odot = 0.0245$. The evolutionary tracks are initialized at the Pre-Main Sequence stage ; therefore, the ages are counted from the ZAMS.

To fit the observational constraints ($T_{\rm eff}$, L and surface metallicity $[Z/X]_{\rm surf}$) with corresponding results of various computations, we adjust the main stellar modeling parameters: mass, age and metallicity. In Fig. 3, the rectangular error boxes correspond to the values and accuracies of the $T_{\rm eff}$ and L parameters quoted in Table 5. The values of the radii reported in the present work select very narrow diagonal sub-areas in these error boxes. The new measurements of radii are thus particularly discriminating for the models, as previously noticed by Thévenin et al. (2005) and Creevey et al. (2007).

We adopt an initial helium content of $Y_{\rm ini} = 0.265$ which correspond to a slightly metal poor disk star. We then tried to fit the evolutionary models within the error boxes of both stars with the masses proposed by Gorshanov et al. (2006) of 0.74 and 0.46 $M_\odot$. In this process, we explored a range of abundance Z/X by changing the observed value by ±0.15 dex and Y by ±0.01 dex. We also tried varying the masses by ±0.05 $M_\odot$. No combination of the three parameters produced evolutionary models reaching the error boxes of the HR diagram, that are strongly constrained by the radius. The variation of the α parameter of the convection depth did not help either. From this we conclude that the masses proposed by Gorshanov et al. (2006) are not reproducible by our modeling within ±0.05 $M_\odot$. For this reason, we decided to use as a starting value the older mass determination by Walker et al. (1995) of 0.67 and 0.59 $M_\odot$. The convergence of our models towards the observations is significantly better and we could refine these masses to the values listed in Table 5.

[1] http://www.marcs.astro.uu.se/

[2] See the documentation of CESAM2k on the Helas website http://helas.group.shef.ac.uk/solar_models.php

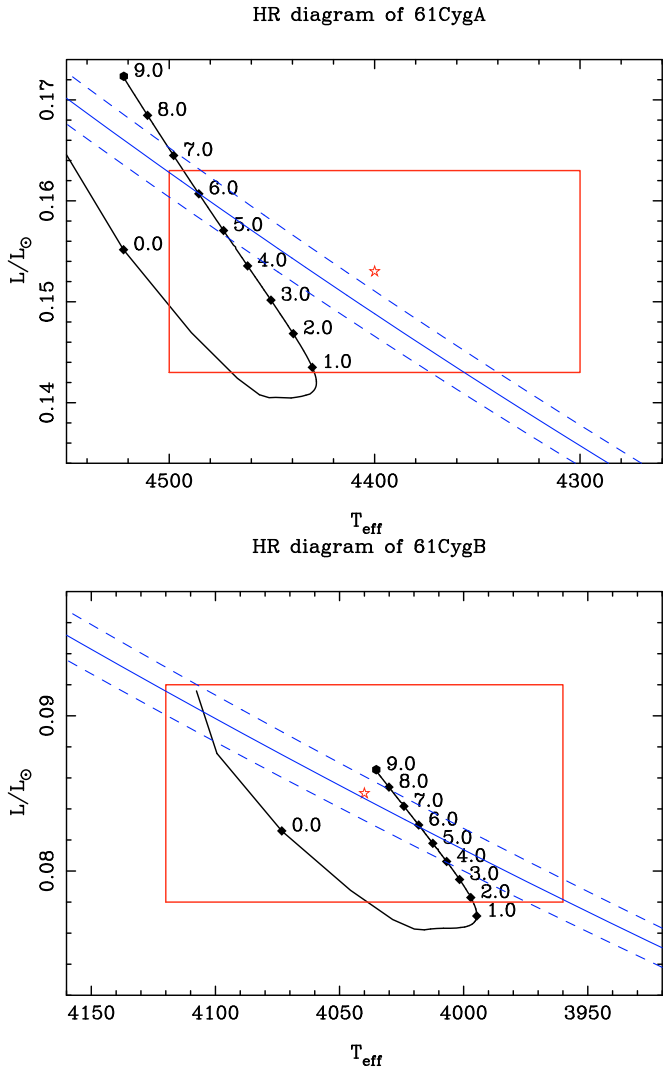

Fig. 3. Evolutionary tracks in the H-R diagram for 61 Cyg A (*top*) and B (*bottom*). The labels indicate the age in Gyr relative to the ZAMS. The rectangular box represents the classical $L - T_{\rm eff}$ error box, and the diagonal lines represent the radius and its uncertainty.

We selected as the most plausible models those satisfying first the luminosity and radius constraints and second the effective temperature constraint. The corresponding parameters are given in Table 5. The models of 61 Cyg A and B converge simultaneously to the radii-limited uncertainty boxes for an age of 6.0 ± 1.0 Gyr. This is significantly older than the 2.1–1.9 Gyr estimate of Barnes (2007), that was derived from the measured rotation period of the stars (gyrochronology). The chromospheric age quoted by this author of 2.4–3.8 Gyr also appears lower than our value.

5. Asteroseismic frequency predictions

Late-type bright binaries are rare but represent, once analysed with asteroseismic constraints, an excellent challenge for internal structure models to derive the age and helium content in the solar neighborhood. With the improved determinations of the fundamental parameters of the 61 Cyg system, we propose predictions of pulsation frequency separations useful for asteroseismic diagnostics. To date, no detection of pulsation has been reported in these two stars. Our purpose here is not to predict

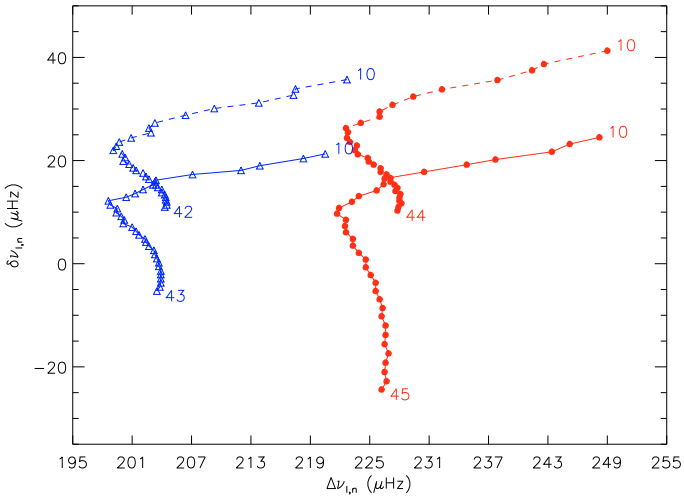

Fig. 4. Diagram representing the small separations $\delta\nu_{n,\ell}$ (vertical axis) as a function of the large ones $\Delta\nu_{n,\ell}$ (horizontal axis) for the two components 61 Cyg A (△) and B (•). We consider here only $(\delta\nu_{n,0}, \Delta\nu_{n,0})$ (solid line) and $(\delta\nu_{n,1}, \Delta\nu_{n,1})$ (dashed line). The successive radial nodes $n > 10$ are indicated on the curves.

which modes are excited but rather to compute a broad range of eigenfrequencies $\nu_{n,\ell}$ with radial orders $n > 10$ and degrees $\ell = 0, 1, 2, 3$ up to the cut-off frequency, so that they will cover possible future detections and eventually help to constrain future models of these stars. For a thourough review of the asteroseismic concepts discussed in the present section, the interested reader is referred to the excellent review by Cunha et al. (2007).

The frequencies $\nu_{n,\ell}$ are calculated with a standard adiabatic code for stellar pulsations (e.g. Unno et al. 1989). Instead of looking at the absolute values of the frequencies, we consider the so-called small $\delta\nu_{n\ell} = \nu_{n,\ell} - \nu_{n-1,\ell+2}$ and large separations $\Delta\nu_{n,\ell} = \nu_{n,\ell} - \nu_{n-1,\ell}$ which are the relevant quantities to constrain stellar properties (e.g. Christensen-Dalsgaard 1984). The former gives information about the stellar evolutionary status of the star since low degree modes have their inner turning points close to or in the core of the star. It is particularly dependent on the gradient of the sound speed in the core which changes as the star evolves (e.g. Gough 1986). The large frequency separation $\Delta\nu_0$ roughly equals:

$$\Delta\nu_0 = \left(2 \int_0^R \frac{\mathrm{d}r}{c_\mathrm{s}}\right)^{-1} \tag{16}$$

with c_s the sound speed. This quantity is a measure of the propagation time inside the star. It is proportional to the mean density which is then a strong constrain on the mass once the radius is determined by interferometry (Cunha et al. 2007). We plot these separations in Fig. 4 in a $(\delta\nu_{n,\ell}, \Delta\nu_{n,\ell})$ diagram for the two components 61 Cyg A & B. The small and large separations show the same behaviors with the radial nodes for the two stars. The shifts between $\Delta\nu_{n,\ell}$ for the two stars reflect the difference of their mean densities. It is interesting to note the change of sign of $\delta\nu_{n,\ell}$ for large values of n.

6. Conclusion

We presented high accuracy interferometric measurements of the angular diameters of the two nearby stars 61 Cyg A & B: $\theta_\mathrm{LD}(\mathrm{A}) = 1.775 \pm 0.013$ mas and $\theta_\mathrm{LD}(\mathrm{B}) = 1.581 \pm 0.022$ mas, corresponding to photospheric radii of $R(\mathrm{A}) = 0.665 \pm 0.005\ R_\odot$ and $R(\mathrm{B}) = 0.595 \pm 0.008\ R_\odot$. We computed CESAM2k models that reproduce these radii as well as the other observed properties of the two stars. 61 Cyg A & B appear as very promising targets for future asteroseismic studies, and we also derived asteroseismic frequencies potentially present in these two stars. The detection of oscillations would bring important constraints to stellar structure models in the cool, low-mass part of the HR diagram, where convection plays a central role. However, in the absence of measured asteroseismic frequencies, it appears difficult to go beyond the present modeling of the binary system. The main reason is that the mass is not constrained sufficiently well by the long period astrometric orbit. We encourage asteroseismic groups to include these two stars in their observing programmes, as the measurement of seismic parameters (in particular the mean large frequency spacing) will bring a decisive constraint to the mass of these stars. We also found that the value of the mixing length parameters for both stars is very well constrained by the radius once the other parameters of the model are fixed, in particular the mass. We reach the same conclusions as Yildiz et al. (2006) that the α parameter is mass dependent at least for solar abundance stars. The future *Gaia* mission (Perryman 2005) will open the way to a complete calibration of several thousand binaries. Such a large sample will give us a completely renewed view of convection in stars (see e.g. Lebreton 2005).

Acknowledgements. The authors would like to thank all the CHARA Array and Mount Wilson Observatory day- time and night-time staff for their support. The CHARA Array was constructed with funding from Georgia State University, the National Science Foundation, the W. M. Keck Foundation, and the David and Lucile Packard Foundation. The CHARA Array is operated by Georgia State University with support from the College of Arts and Sciences, from the Research Program Enhancement Fund administered by the Vice President for Research, and from the National Science Foundation under NSF Grant AST 0606958. This work also received the support of PHASE, the high angular resolution partnership between ONERA, Observatoire de Paris, CNRS and University Denis Diderot Paris 7. This research took advantage of the SIMBAD and VIZIER databases at the CDS, Strasbourg (France), and NASA's Astrophysics Data System Bibliographic Services.

References

Affer, L., Micela, G., Morel, T., Sanz-Forcada, J., & Favata, F. 2005, A&A, 433, 647
Aufdenberg, J. P., Ludwig, H. G., & Kervella, P. 2005, ApJ, 633, 424
Alonso, A., Arribas, S., & Martínez-Roger, C. 1996, A&A, 313, 873
Baize, P. 1950, Journal des Observateurs, 33, 1
Baraffe, I., Chabrier, G., Barman, T. S., Allard, F., & Hauschildt, P. H. 2003, A&A, 402, 701
Barnes, S. A. 2007, ApJ, 669, 1167
Bessel, F. W. 1838, MNRAS, 4, 152
Bigot, L., Kervella, P., Thévenin, F., & Ségransan, D. 2006, A&A, 446, 635
Böhm-Vitense, E. 2007, ApJ, 657, 486
Burgers, J. M., 1969, Flow Equations for Composite Gases (New York Academic Press)
Cester, B., Ferluga, S., & Boehm, C. 1988, Ap&SS, 96, 125
Christensen-Dalsgaard, J., 1984, Space Research Prospects in Stellar Activity and Variability, ed. A. Mangeney, & F. Praderie (Paris Observatory Press), 11
Claret, A., 2000, A&A, 363, 1081
Coudé du Foresto, V., Ridgway, S., & Mariotti, J.-M. 1997, A&AS, 121, 379
Coudé du Foresto, V., Bordé, P., Mérand, A., et al. 2003, Proc. SPIE, 4838, 280
Creevey, O. L., Monteiro, M. J. P. F. G., Metcalfe, T. S., et al. 2007, ApJ, 659, 616
Cunha M. S., Aerts C., Christensen-Dalsgaard J., et al. 2007, A&ARv, 14, 217
Deich, A. N. 1978, Pis'ma Astron. Zh., 4, 95
Deich, A. N., & Orlova, O. N. 1977, Astron. Zh., 54, 327
Ducati, J. R. 2002, NASA Ref. Pub., 1294
ESA 1997, The Hipparcos and Tycho Catalogues, ESA SP-1200
Grevesse, N., & Noels A. 1993, Cosmic Abundances of the Elements, ed. N. Prantzos, E. Vangioni-Flam, & M. Cassé, Origin and Evolution of the Elements (Cambridge University Press), 14
Gorshanov, D. L., Shakht, N. A., & Kisselev, A. A. 2006, Ap, 49, 386

Gough, D. O., 1986, in Hydrodynamic and magnetohydrodynamic problems in the Sun and stars, ed. Y. Osaki, Department of Astronomy, University of Tokyo, 117
Gustafsson, B., Bell, R. A., Eriksson, K., & Nordlund, Å. 1975, A&A, 42, 407
Gustafsson, B., Edvardsson, B., Eriksson, et al. 2003, ASP Conf. Ser. 288, ed. I. Hubeny, D. Mihalas, & K. Werner, 331
Gustafsson, B., Heiter, U., & Edvardsson, B. 2007, IAU Symp. 241, ed. A. Vazdekis, & R. F. Peletier, 47
Gustafsson, B., Edvardsson B., Eriksson K., et al. 2008, A&A, 486, 951
Hall, J. C., Lockwood, G. W., & Skiff, B. A. 2007, AJ, 133, 862
Hestroffer, D., & Magnant, C. 1998, A&A, 333, 338
Hempelmann, A., Robrade, J., Schmitt, J. H. M. M., et al. 2006, A&A, 460, 261
Houdashelt, M. L., Bell, R. A., & Sweigart, A. V. 2000, AJ, 119, 1448
Kervella, P., Thévenin, F., Ségransan, D., et al. 2003a, A&A, 404, 1087
Kervella, P., Thévenin, F., Morel, P., Bordé, P., & Di Folco E. 2003b, A&A, 408, 681
Kervella, P., Ségransan, D. & Coudé du Foresto, V. 2004a, A&A, 425, 1161
Kervella, P., Thévenin, F., Di Folco E., & Ségransan, D. 2004b, A&A, 426, 297
Lane, B. F., & Colavita, M. M. 2003, AJ, 125, 1623
Lebreton, Y. 2005, ESA SP-576, 493
Luck, R. E., & Heiter, U. 2005, AJ, 129, 1063
Luck, R. E., & Heiter, U. 2006, AJ, 131, 3069
Mérand, A., Bordé, P., & Coudé du Foresto, V. 2005, A&A, 433, 1155
Mérand, A., Coudé du Foresto, V., Kellerer, A., et al. 2006, Proc. SPIE, 6268, 46
Mérand, A., et al. 2008, in preparation
Morel, P., 1997, A&AS, 124, 597
Morel, P., & Lebreton, Y. 2007, Ap&SS, doi:10.1007/s10509-007-9663-9
Morel, P., & Thévenin, F. 2002, A&A, 390, 611
Morel, P., Pichon, B., Provost, J., & Berthomieu, G. 1999, A&A, 350, 275
Paquette, C., Pelletier, C., Fontaine, G., & Michaud, G. 1986, ApJS, 61, 177
Perrin, G., 2003, A&A, 400, 1173
Perryman, M., 2005, ESA SP-576, 15
Skrutskie, R. M., Cutri, R., Stiening, M. D., et al. 2006, AJ, 131, 1163
Strand, K. A. 1943, Proc. Am. Phil. Soc., 86, 364
Strand, K. A. 1957, AJ, 62, 35
ten Brummelaar, T. A., Mc Alister, H. A., Ridgway, S. T., et al. 2005, ApJ, 628, 453
Thévenin, F., Provost, J., Morel, P., et al. 2002, A&A, 392, L9
Thévenin, F., Kervella, P., Pichon, B., Morel, P., et al. 2005, A&A, 436, 253
Tomkin, J., & Lambert, D. L. 1999, ApJ, 523, 234
Unno, W., Osaki, Y., Ando, H., Saio, H., & Shibahashi, H., 1989, Nonradial Oscillations of Stars, 2nd edn., (University of Tokyo Press)
Van Altena, W. F., Lee, J. T., & Hoffleit, E. D. 1995, The General Catalogue of Trigonometric Stellar Parallaxes, 4th edition, Yale University Observatory
van de Kamp, P. 1953, AJ, 58, 21
van de Kamp, P. 1954, AJ, 59, 447
van de Kamp, P. 1973, AJ, 78, 1099
van Leeuwen, F. 2007a, Hipparcos, the New Reduction of the Raw Data, Astrophysics and Space Science Library (Springer), 350
van Leeuwen, F. 2007b, A&A, 474, 653
Walker, G. A. H., Walker, A. R., Irwin, A. W. et al. 1995, Icarus, 116, 359
Worley, C. W., & Heintz, A. D. 1983, Fourth Catalogue of Orbits of Visual Binary Stars
Yildiz, M., Yakut, K., Baakis, H., & Noels, A. 2006, MNRAS, 368, 1941
Zagar, F. 1934, Atti R. Ist. Veneto di Sc. L. A., 94, 259
Zboril, M., & Byrne, P. B. 1998, MNRAS, 299, 753